Published by :
http://www.ijert.org

International Journal of Engineering Research & Technology (IJERT)
ISSN: 2278-0181
Vol. 9 Issue 02, February-2020

Investigation of Structural, Morphological and Optical Properties of Mn and Fe Co-Doped ZnO Thin Films Prepared by Spray Pyrolysis Process

Md. Khalid Hasan*, Md. Zahidul Islam*, Nur Mohammad Shehab*, Md. Saifur Rahman*
*Department of Glass & Ceramic Engineering, RUET,
Rajshahi-6204, Bangladesh

Abstract: **Mn & Fe doped ZnO thin films were prepared by low-cost spray pyrolysis method and the influence of co-dopants on the structural, morphological and optical properties has been studied. The X-ray diffraction analysis reveals that Mn & Fe co-doping has a significant effect on crystalline quality, grain size, strain in thin films. SEM and XRD study showed that 3% Mn & Fe co-doped has the best crystalline quality. Also, the XRD study showed that deposited thin film has a polycrystalline wurtzite structure with a minor amount of impurity. The effect of the impurity phase on morphological and optical properties has also been studied. Other optical parameters like absorption coefficient, transmittance, absorbance, and optical bandgap have also been determined. Obtained photoluminescence results showed that higher percent doping increases defects. Obtained results indicate that the thin films of Mn & Fe doped ZnO are a potential candidate for use in optical limiters and optical switching devices.**

Keywords: ***ZnO thin films; Microstructure; Band gap; Transmittance***

1. INTRODUCTION

Nano crystalline semiconductor materials have a great significance due to their extraordinary structural stability as well as wide bandgap property. Zinc oxide is one of the most important and versatile oxide materials due to its high transparency in the visible range, direct bandgap (3.37ev), absence of toxicity, high electrochemical stability, abundance in nature, etc [1]. Zinc oxide (ZnO) is one of the most attractive materials which has been developing recently to use in microelectronic application [2]. It is also used in developing new optoelectronic devices

such as solar cell windows, piezoelectric transducers, gas sensors, ultraviolet (UV) lasers, short-wavelength light-emitting diodes, photodetectors, etc [3]. Zinc oxide (ZnO), having a wide bandgap has a stable hexagonal wurtzite structure and is composed of alternating planes with tetrahedrally coordinated O^{2-} and Zn^{2+} ions [4]. ZnO thin films can be prepared by different deposition techniques. The various deposition techniques are spray pyrolysis [5], chemical vapor deposition [6], electron beam evaporation [7], molecular beam epitaxy [8], and pulsed laser deposition [9]. Among them in the present study, we have performed a simple and cost-effective spray pyrolysis method.

ZnO is one of the oxide materials in which Mn^{2+} (0.66 Å) dopant having similar radius replace Zn^{2+}(0.60 Å) without any phase segregation and assumed to be a deep donor with energy levels as 0.45, 0.7 or 2.0ev below the conduction band edge at room temperature [14, 10]. Besides doping with transition metal could affect the electronic band structure of ZnO and may change its applications [11, 12, 13]. Besides various transition elements such as Ni, Cr, Cu, Co, Ti, V, etc. are also tried as dopants into the ZnO matrix to further improve its optical and electrical behavior. Among various dopants, Fe dopant into ZnO matrix has less explored by spray pyrolysis technique. Moreover, it has also a similar radius compared to Zn^{2+} which also can substitute the Zn^{2+} into ZnO. Adding 3d transition metal into ZnO matrix may change the fermi energy state by raising valence band to maximum and lowering conduction band to minimum, thus lowering the bandgap. Thus, it is expected form the study that the bandgap would be lowered due to co-doping of 3d transition element Mn & Fe. Moreover, Salaken et. al explored that lower or higher Fe dopants degrade the optical and crystalline quality [15]. So, it will be interesting to see the mixed effect of Mn & Fe co-dopants into the ZnO matrix. Another challenge of the study was single phase formation. However, possible impurities and their effects on optical properties has also been described.

2. MATERIALS AND METHOD

ZnO thin film was prepared by spraying of zinc acetate (Zn $(CH_3COO)_2.2H_2O$, analytical grade) in a mixture of deionized water and isopropyl alcohol (2:3 by volume) onto heated glass substrates. The glass substrate was placed on a soldered tin bath. In our experiment, we use $(CH_3COO)_2Zn.2H_2O$), Mn $(NO_3)_2{\cdot}4H_2O$, $FeCl_3$, (Merck India), HCl, Sigma Aldrich as primary raw material. To prepare a solution, appropriate amount of each element was calculated and mixed with 200ml water. For complete dissolution, few drops of HCl were added. Similarly, for DZO-3, DZO-5, DZO-7 (DZO referred to Mn & Fe doped ZnO thin films) films with required ingredients were weighed and solution concentration was kept in 0.12 M level. After that, the prepared solution was filtered with a filter paper with the help of a funnel. Several parameters were controlled such as temperature, airflow, solution flow rate during the deposition process. At first, all the parameters were adjusted and then the mild steel mask was set upon the glass substrate. After that, the substrate was taken over a steel plate. Then the plate was placed over the heater. Subsequently, the current supply was switched on and the heating rate was changed by varying the voltage. Then the prepared solution was pouring

International Journal of Engineering Research & Technology (IJERT)
ISSN: 2278-0181
Vol. 9 Issue 02, February-2020

into the measuring cylinder that was attached to buerrete stand with the clamp. The solution was taken out through the tube of commercial saline set and passed it to the inlet of the nozzle. During film deposition, the temperature of the substrate was raised to 350 °C by varying voltage. The rate of flow of solution was controlled manually in our desired level. As around 5 ml solution was sprayed to the substrate within 10 minutes, the supply of heat, air, and solution were stopped then and the film was kept untouched for cooling 5-10 minutes. After that, the deposited film samples were wrapped in tracing paper and stored for XRD, SEM, UV-Vis. Characterization.

3. RESULT AND DISCUSSION

STRUCTURAL ANALYSIS

X-ray diffraction analysis (XRD) was done to acquire structural information. The room temperature XRD curve is shown in Fig. 1. All the XRD peaks of each pattern could be indexed to monophasic zinc oxide hexagonal wurtzite structure according to JCPDS card number 36-1451. The XRD patterns of both doped and undoped samples along (100), (002) and (101) planes exhibited strong orientation. The calculated lattice parameters are found to be a = b = 3.25 Å, c = 5.2 Å, V= 47.567 $Å^3$ which is a complete agreement to the previous standard study [16]. It may be mentioned that the lattice parameters have changed due to the co-doping. Moreover, Rietveld refinement was done to analyze the XRD patterns. This was done using Fullprof software. It was found that the hexagonal wurtzite type structure was best suited for both undoped and doped samples. The calculated data are tabulated in Table 1.

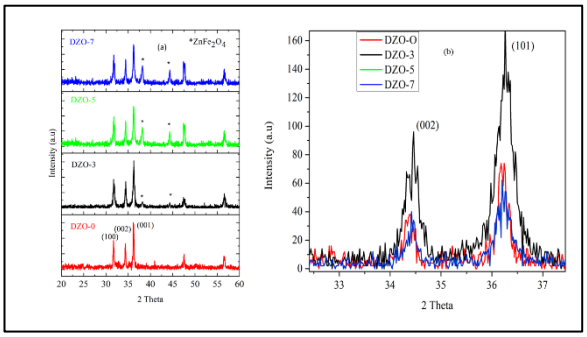

Fig. 1: (a) Room temperature XRD patterns of DZO-(0, 3, 5, 7) thin films; (b) Magnified patterns in the range of (33-37) °

Increasing volume indicates the perfect doping of elements into the ZnO matrix. Furthermore, the intensities along different diffraction peaks are different, which indicates that the growth of ZnO in

Table 1: Structural parameters of DZO-(0, 3, 5, 7) thin films obtained by Reitveld refinement.

Parameters	Sample			
	DZO-0	DZO-3	DZO-5	DZO-7
a (Å)	3.2414	3.255	3.214	3.142
c (Å)	5.211	5.2175	5.191	5.11
d_{100} (Å)	2.771	2.819	2.783	2.760
V ($Å^3$)	47.41	47.889	46.44	45.323
Density g/cm^3	6.051	5.644	5.82	6.06
Dislocation density (δ) *10^{15} lines/m^2	11.79	13.09	15.96	19.37
Strain (ε) *10^{-3}	3.26	3.39	3.74	4.2
Chi^2	2.01	2.5	2.23	2.65
R_{exp}	17	12.79	13	10.6

various planes are different and the growth is anisotropic. The observed Rietveld XRD patterns in Fig. 2 indicate a differential crystallinity with a minor amount of impurity phase, $ZnFe_2O_4$.

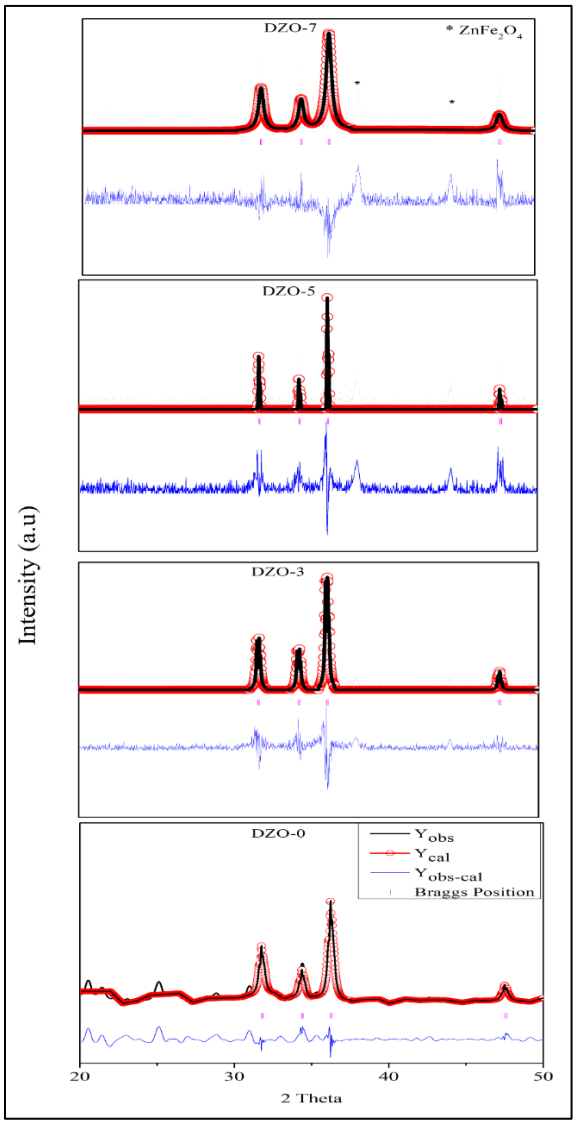

Fig. 2: Reitveld refined XRD pattern of DZO-(0, 3, 5, 7) thin films.

International Journal of Engineering Research & Technology (IJERT)
ISSN: 2278-0181
Vol. 9 Issue 02, February-2020

It has been found from Fig. 3 that the average grain size reduces due to doping which may support the reduction of intensity along (002) planes due to doping.

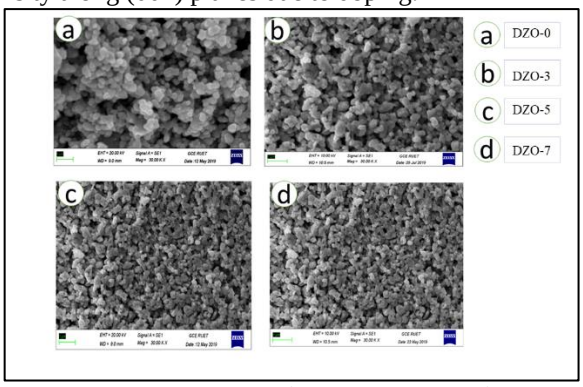

Fig. 3: SEM micrographs of DZO-(0, 3, 5, 7) thin films.

Average grain size values are tabulated in Table 2.

From the recorded X-ray diffraction data, the grain size of crystallites was calculated using Scherer's equation [18]:

$$D = \frac{0.9\lambda}{\beta cos\theta} \quad (1)$$

Where D is the grain size of the crystallites, λ is the wavelength of X-rays, β is the full width half maxima and θ is the angle of diffraction. The calculated crystallite size values are tabulated in Table 2**.** Reduction of average grain size indicates merging from good crystallinity [19].

Table 2: Crystallite size and Average grain size of DZO-(0, 3, 5, 7) thin films.

Name of the element	Crystallite Size (nm)	Average grain size (nm)
DZO-0	29.12	58.83
DZO-3	27.63	51.52
DZO-5	25.03	46.61
DZO-7	22.72	44.88

As with higher doping of 5 and 7%, peaks intensity falls down with high background noise which indicates reducing crystallinity and inducing stress. Annealed stress released samples may show improved crystallinity [20].

From the present study, dislocation density (δ) and lattice strain of estimated samples are calculated using following equation [21]:

$$\delta = n/D^2 \quad (2)$$

Where n = 1, indicates the minimum dislocation density of the film and D is the calculated crystallite size. The dislocation density of any material provides the quality of films and its defect structure of the material. The dislocation density usually is defined as the number of dislocations per unit length or per unit area of desired samples [22]. In the present study, incorporation of Mn and Fe doping in The ZnO matrix, the dislocation density gradually increases which indicates its defect structure. The lattice strain was calculated using the following equation [21] and shows similar trend with exactly to the dislocation density.

$$\varepsilon = \frac{\beta \cos\theta}{4} \quad (3)$$

The lattice strain data are tabulated in Table 1.

3.1 MORPHOLOGICAL ANALYSIS

Surface morphological studies of the DZO-0, DZO-3, DZO-5 & DZO-7 films were carried out by scanning electron micrographs (SEM). Fig. 3 (a-d) shows the SEM images of all the undoped and doped ZnO thin films. The microstructure of DZO-0 thin-film clearly shows that grains are round in shape. Careful observation indicates the roughness of the surface and the presence of a significant amount of porosity. It is seen from the SEM Fig. 3 that porosity content and surface roughness increase with increasing Mn and Fe doping concentration. But for DZO-3 thin film, the roughness was minimal compared to the other two dopant concentrations.

Another lucid visualization from the SEM graph indicates increasing the doping percentage causes a gradual decrease in average grain size. The average grain size was calculated using the linear intercept formula [23]. The calculated average grain size was tabulated in Table 2**.** In our present study, increasing doping percentages cause a decrease in interstitial Zinc due to the dopant's concentration. Therefore, the grin growth of ZnO was inhibited due to the decreasing of diffusivity [24]. Besides, difference of ionic radius between Fe^{+x} (x = +2 or +3), Zn^{2+} as well as between Mn^{2+} and Zn^{2+}, where both Fe^{+x} & Mn^{2+} replaces Zn^{2+} in ZnO matrix causes lattice distortion, resulting in larger strain and subsequently hinder the grain growth [15, 17]. However, in our case, we have used $FeCl_3$ as our source for the experiment. So, lattice distortion occurred due to the replacement of Fe^{3+} to Zn^{2+} in the ZnO matrix, which is another source for grain growth inhibitor [24]. The grain size distribution of DZO thin films was depicted by histogram graph as in Fig. 4. Also, the lucid visualization of histogram data is a good agreement with SEM data. Therefore, the study reveals that increasing the co-doping percentage causes a gradual decrease in grain size.

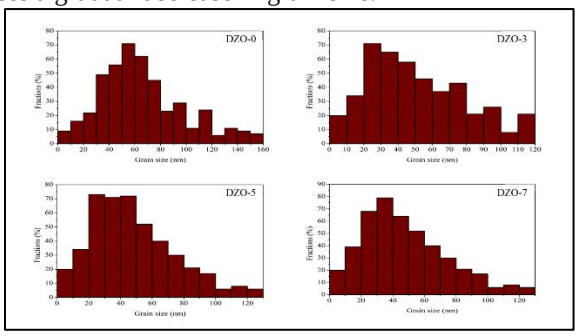

Fig. 4: Grain size distribution of DZO-(0, 3, 5, 7) thin films.

3.2 OPTICAL PROPERTY ANALYSIS

The optical transmission spectra of both Mn & Fe doped and undoped ZnO thin films of 0.69 μm are showed in Fig. 5**.** The optical transmission is found to be maximum for 7% Mn & Fe doped ZnO in the range between 400-750 nm. At higher wavelengths from visible to IR region of all films, there are high transmittance, low absorbance, and reflectance which indicates that present samples have large transmittance windows for optical applications [19]. Therefore, DZO-3 shows the highest transmittance performance

International Journal of Engineering Research & Technology (IJERT)
ISSN: 2278-0181
Vol. 9 Issue 02, February-2020

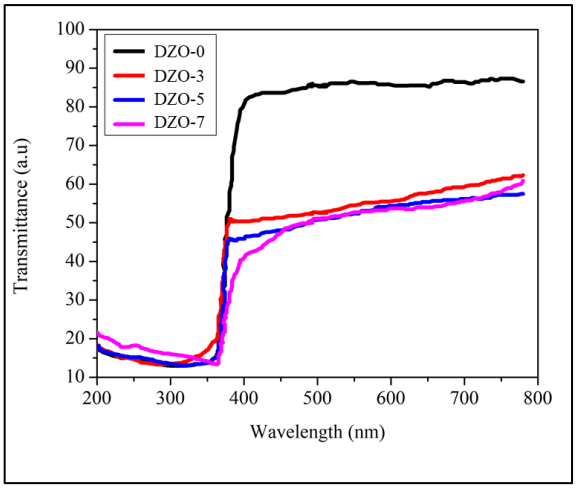

Fig. 5: Transmittance spectra of DZO-(0, 3, 5, 7) thin films.

among other Mn & Fe doped thin films due to less light scattering and thus it can be exclusively used in solar cells [25]. In the present study, defect structure may contribute to the less transmittance of DZO-5 & DZO-7 thin films. Some researchers found that defect structure may hinder the transmittance of thin films [26]. The absorbance spectra of both doped and undoped ZnO thin films are showed in Fig. 6.

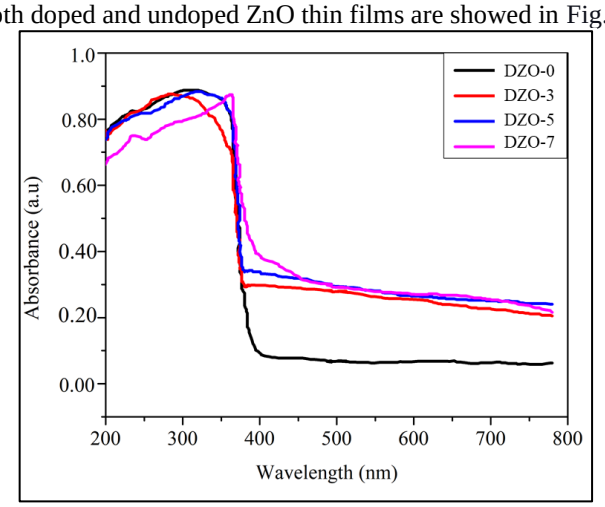

Fig. 6: Absorbance spectra of DZO-(0, 3, 5, 7) thin films.

The absorbance spectra showed that absorbance increased in the visible range with slightly increasing the doping percentage. This may be attributed to the introduction of defect states within the forbidden band in the case of DZO-5 and DZO-7 films, which may lead to the absorption of incident photons [14].

The optical band gap (E_g) for the deposited films was calculated on the basis of spectral absorption for ZnO. The direct band gap of material is calculated using the Tauc's relation,

$$\alpha h\upsilon = A\left(h\upsilon - E_g\right)^{\frac{1}{2}} \qquad (4)$$

where $h\upsilon$ is the incident photon energy, A is constant of energy for a material within the measured optical material frequency range, Eg is the energy gap between the valance and conduction band. The band gap has been calculated by extrapolating the linear region of the plots $(\alpha h\upsilon)^2$ versus hυ on the energy axis as shown in Fig. 7.

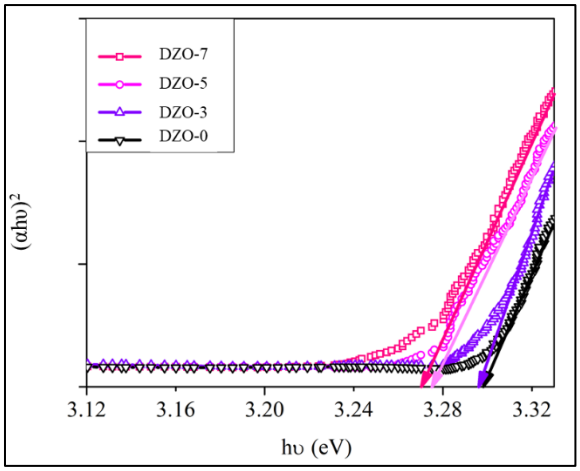

Fig. 7: Band gap of DZO-(0, 3, 5, 7) thin films.

The optical band gap of material depends on many properties such as defects, type of materials, absorption coefficient [27]. Those materials which have a high bandgap is very useful for solar cell application as well as optoelectronic application [28]. From Fig. 7 we found that increasing dopant percent decreases the bandgap slightly. Such a widening of the optical band gap with co-doping where an enhancement of n-type carrier concentration occurred in ZnO structure due to (Fe^{3+} doping) can be well described by Burstein–Moss effect [29]. By enhancement of n-type carrier concentration with doping; absorption edge forms at much shorter wavelengths than intrinsic samples and lowers the Fermi level down into the conduction band which widens the bandgap. This is well-known as the Burstein–Moss effect [29]. The decreasing trend of bandgap with increasing Fe & Mn concentration may be attributed that, 3d transition metal ions into ZnO layers may change the Fermi energy state by lifting the valence band to a maximum and lowering the conduction band minimum leading to bandgap reduction. Moreover, it is also attributed that, narrowing of bandgap may be attributed to the strong s-d and p-d spin-exchange interactions between the band electrons and the localized d electrons of Fe^{3+} & Mn^{2+} ions substituting Zn^{2+} ions as mentioned by Srinivasulu et al. [30] for FZO thin films prepared by chemical spray pyrolysis. Bandgap values are tabulated in Table 3**.**

Table 3: Band gap of DZO-(0, 3, 5, 7) thin films.

Name of the element	Band gap (eV)
DZO-0	3.30
DZO-3	3.29
DZO-5	3.275
DZO-7	3.265

The refractive index and absorption coefficient of these films were determined using transmittance and reflectance measurements. The refractive index, (n) has been calculated using the relation [31], showed in Fig. 8,

International Journal of Engineering Research & Technology (IJERT)
ISSN: 2278-0181
Vol. 9 Issue 02, February-2020

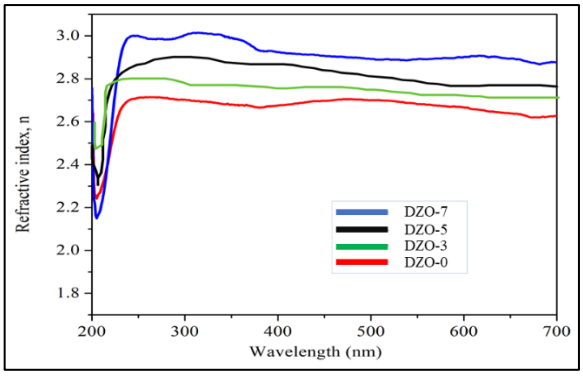

Fig. 8: Refractive index of DZO-(0, 3, 5, 7) thin films.

$$n = \frac{(1+R)}{(1-R)} + \sqrt{\left(\frac{4R}{(1-R)^2} - k^2\right)} \qquad (5)$$

As well as, refractive index is found to increase with the addition of Mn & Fe dopants. This may be due to the change in crystallite size, stoichiometry and internal strain with the addition of various sizes dopants to the Zn-O network [32,33]. It has been observed that an overall decreasing trend for the refractive index with the photon energy shifting to the higher value that is towards the lower value of wave length. It has been found for all the samples that an overall increase in the refractive index towards the larger wavelength in the visible region.

The absorption coefficients (k) of the samples were calculated from the following relation [34],

$$k = \frac{\alpha\lambda}{4\pi} \qquad (6)$$

Fig. 9 shows the plots of absorption coefficients (k) versus wavelength of pure and doped thin films.

In the present study, the absorption coefficients (k) values are varying between ~ 0.34 to 0.38. Which shows the influence of co-doping on ZnO thin films. Further, the value indicates that the material has defects which are also confirmed by dislocation density and Rietveld analysis already. In the visible range at the higher wavelength, the absorption coefficient(k) remains constant upon doping. Lower values of k indicate that it can be suitable for various optical applications [35].

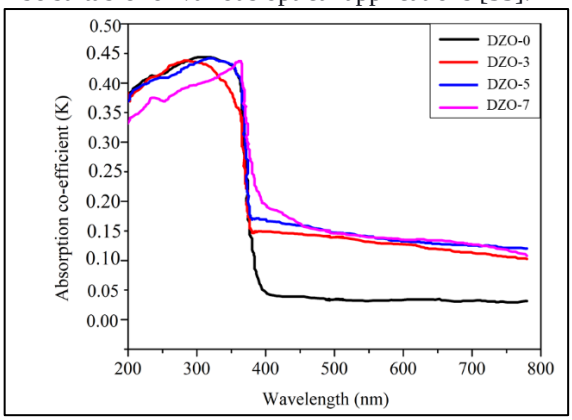

Fig. 9: Absorption co-efficient of DZO-(0, 3, 5, 7) thin films.

Fig. 10 shows the photoluminescence spectra of undoped and Mn & Fe doped ZnO thin films at room temperature under the excitation of 325 nm.

From the Fig. 10, it is found that the strongest ultraviolet emission peak centered at 373 nm corresponds to near band emission (NBE). There are three peaks observed nearly at 398 nm, 467 nm and 477 nm which are attributed to various intrinsic defects such as Zinc interstitials and doubly ionized oxygen or both effects. We have identified that the intensity of the NBE peak is high for the sample obtained with 3% Mn & Fe doped ZnO thin films. This can be explained by the fact that it has very a smaller number of defects and higher crystallinity compared to DZO-7 and DZO-0 thin films. The NBE peak of DZO-7 has very lower intensity due to the presence of a larger number of defects which is already proved in the Reitveld refinement [36].

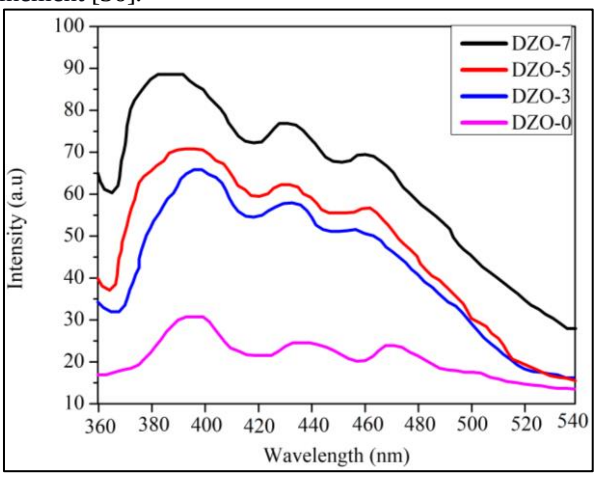

Fig. 10: Photoluminescent spectra of DZO-(0, 3, 5, 7) thin films.

4. CONCLUSION

Undoped ZnO and doped ZnO thin films with different doping concentrations (3, 5 and 7 at%) of Mn & Fe have been successfully deposited on glass substrate using spray pyrolysis technique. All the thin films exhibit hexagonal wurtzite type with additional $ZnFe_2O_4$ as a secondary (impurity) phase for 3%, 5%, and 7% doping. A minor amount of impurity has a significant effect on the properties of the ZnO thin film. The values of crystallite and grain size both are found to be decreased with increasing doping concentrations. The UV-vis spectroscopy was done to confirm the high transparency. For 3% doping, the transmittance was higher. The optical band gap was calculated for all films and found a gradually decreasing trend for higher percent doping which can be useful for solar cell applications. Photoluminescence spectra showed that it has a very smaller number of defects at DZO-3. From the optical data, we have also calculated the absorption index, refractive index. In the visible range, at the higher wavelength, the absorption index (k) remains constant upon co-doping which indicates it can be suitable for various optical and optoelectronic applications.

International Journal of Engineering Research & Technology (IJERT)
ISSN: 2278-0181
Vol. 9 Issue 02, February-2020

5. ACKNOWLEDGEMENT

The authors would like to thank Rajshahi University of Engineering & Technology for producing necessary testing facilities. This research did not receive any specific grant from funding agencies in the public, commercial, or not-for-profit sectors.

REFERENCES

[1] Ismail, B., Abaab, M. and Rezig, B. "Structural and electrical properties of ZnO films prepared by screen printing technique." Thin Solid Films, vol.383(1-2), pp. 92-94, 2001

[2] Rusu, G.I., Ciupina, V., Popa, M.E., Prodan, G., Rusu, G.G. and Baban, C. "Microstructural characterization and optical properties of ZnSe thin films." Journal of non-crystalline solids, vol. 352(9-20), pp. 1525-1528, 2006

[3] Zhang, T.C., Mei, Z.X., Guo, Y., Xue, Q.K. and Du, X.L. "Influence of growth temperature on formation of continuous Ag thin film on ZnO surface by ultra-high vacuum deposition." Journal of Physics D: Applied Physics, vol. 42(11), pp. 119801, 2009

[4] Klingshirn, C. "The luminescence of ZnO under high one-and two-quantum excitation." physica status solidi (b), vol. 71(2), pp. 547-556, 1975

[5] Fiddes, A.J.C., Durose, K., Brinkman, A.W., Woods, J., Coates, P.D. and Banister, A.J. "Preparation of ZnO films by spray pyrolysis." Journal of crystal growth, vol.159(1-4), pp.210-213, 1996

[6] Natsume, Y., Sakata, H., Hirayama, T. and Yanagida, H. "Low-temperature conductivity of ZnO films prepared by chemical vapor deposition." Journal of applied physics, vol. 72(9), pp.4203-4207, 1992

[7] Sahu, D.R., Lin, S.Y. and Huang, J.L. "Improved properties of Al-doped ZnO film by electron beam evaporation technique." Microelectronics Journal, vol. 38(2), pp. 245-250, 2007

[8] Ong, C.K. and Wang, S.J. "In situ RHEED monitor of the growth of epitaxial anatase TiO2 thin films." Applied surface science, vol.185(1-2), pp. 47-51, 2001

[9] Craciun, V., Elders, J., Gardeniers, J.G.E. and Boyd, I.W. "Characteristics of high quality ZnO thin films deposited by pulsed laser deposition." Applied physics letters, vol.65(23), pp. 2963-2965, 1994

[10] Kim, S.S., Moon, J.H., Lee, B.T., Song, O.S. and Je, J.H. "Heteroepitaxial growth behavior of Mn-doped ZnO thin films on Al 2 O 3 (0001) by pulsed laser deposition." Journal of applied physics, vol. 95(2), pp. 454-459, 2004

[11] Donkova, B., Dimitrov, D., Kostadinov, M., Mitkova, E. and Mehandjiev, D. "Catalytic and photocatalytic activity of lightly doped catalysts M: ZnO (M= Cu, Mn)." Materials Chemistry and Physics, vol.123(2-3), pp. 563-568, 2010

[12] Ashokkumar, M. and Muthukumaran, S. "Enhanced room temperature ferromagnetism and photoluminescence behavior of Cu-doped ZnO co-doped with Mn." Physica E: Low-Dimensional Systems and Nanostructures, vol. 69, pp. 354-359 2015

[13] Srinivasulu, T., Saritha, K. and Reddy, K.R. "Synthesis and characterization of Fe-doped ZnO thin films deposited by chemical spray pyrolysis." Modern Electronic Materials, vol. 3(2), pp. 76-85, 2017

[14] Shinde, V.R., Gujar, T.P., Lokhande, C.D., Mane, R.S. and Han, S.H. "Mn doped and undoped ZnO films: A comparative structural, optical and electrical properties study." Materials Chemistry and Physics, vol.96(2-3), pp. 326-330, 2006

[15] Salaken, S.M., Farzana, E. and Podder, J. "Effect of Fe-doping on the structural and optical properties of ZnO thin films prepared by spray pyrolysis." Journal of Semiconductors, vol. 34(7), pp.073003, 2013

[16] Özgür, Ü., Alivov, Y.I., Liu, C., Teke, A., Reshchikov, M., Doğan, S., Avrutin, V.C.S.J., Cho, S.J. and Morkoç, A.H. "A comprehensive review of ZnO materials and devices." Journal of applied physics, vol. 98(4), pp. 11, 2005

[17] Suwanboon, S., Ratana, T. and Ratana, T. "Effects of Al and Mn dopant on structural and optical properties of ZnO thin film prepared by sol-gel route." Walailak Journal of Science and Technology (WJST), vol. 4(1), pp. 111-121, 2007

[18] Cullity, B.D. "Elements of X-ray diffraction", MA. Massachusetts: Addison-Wesley, vol.359, (1978)

[19] Ganesh, V., Yahia, I.S., AlFaify, S. and Shkir, M. "Sn-doped ZnO nanocrystalline thin films with enhanced linear and nonlinear optical properties for optoelectronic applications." Journal of Physics and Chemistry of Solids, vol. 100, pp. 115-125, 2017

[20] Lee, Y.C., Hu, S.Y., Water, W., Tiong, K.K., Feng, Z.C., Chen, Y.T., Huang, J.C., Lee, J.W., Huang, C.C., Shen, J.L. and Cheng, M.H. "Rapid thermal annealing effects on the structural and optical properties of ZnO films deposited on Si substrates." Journal of Luminescence, vol.129(2), pp. 148-152, 2009

[21] Saha, S. and Gupta, V. "Al and Fe co-doped transparent conducting ZnO thin film for mediator-less biosensing application." AIP Advances, vol. 1(4), pp. 042112, 2011

[22] Usha, K.S., Sivakumar, R. and Sanjeeviraja, C. "Optical constants and dispersion energy parameters of NiO thin films prepared by radio frequency magnetron sputtering technique." Journal of Applied Physics, vol.114(12), pp. 123501, 2013

[23] Abrams, H. "Grain size measurement by the intercept method." Metallography, vol.4(1), pp. 59-78, 1971

[24] Fujihara, S., Sasaki, C. and Kimura, T. "Effects of Li and Mg doping on microstructure and properties of sol-gel ZnO thin films." Journal of the European Ceramic Society, vol.21(10-11), pp. 2109-2112, 2001

[25] Reddy, N.N.K., Akkera, H.S., Sekhar, M.C. and Park, S.H. "Zr-doped SnO 2 thin films synthesized by spray pyrolysis technique for barrier layers in solar cells." Applied Physics A, vol.123(12), pp. 761, 2017

[26] Sun, R.D., Nakajima, A., Fujishima, A., Watanabe, T. and Hashimoto, K. "Photoinduced surface wettability conversion of ZnO and TiO2 thin films." The Journal of Physical Chemistry B, vol.105(10), pp.1984-1990, 2001

[27] Zeng, H., Duan, G., Li, Y., Yang, S., Xu, X. and Cai, W. "Blue Luminescence of ZnO nanoparticles based on non-equilibrium processes: defect origins and emission controls." Advanced Functional Materials, vol.20(4), pp. 561-572, 2010

[28] Sernelius, B.E., Berggren, K.F., Jin, Z.C., Hamberg, I. and Granqvist, C.G. "Band-gap tailoring of ZnO by means of heavy Al doping." Physical Review B, vol. 37(17), pp. 10244, 1988

[29] Moss, T.S. "The interpretation of the properties of indium antimonide." Proceedings of the Physical Society. Section B, vol. 67(10), pp. 775, 1954

[30] Srinivasulu, T., Saritha, K. and Reddy, K.R. "Synthesis and characterization of Fe-doped ZnO thin films deposited by chemical spray pyrolysis." Modern Electronic Materials, vol. 3(2), pp. 76-85, 2017

[31] Gadallah, A.S. and El-Nahass, M.M. "Structural, optical constants and photoluminescence of ZnO thin films grown by sol-gel spin coating." Advances in Condensed Matter Physics, (2013)

[32] Tepehan, F. and Özer, N. "A simple method for the determination of the optical constants, n and k of cadmium sulfide films from transmittance measurements." Solar energy materials and solar cells, vol. 30(4), pp. 353-365, 1993

[33] Ashour, A., El-Kadry, N. and Mahmoud, S.A. "On the electrical and optical properties of CdS films thermally deposited by a modified source." Thin solid films, vol. 269(1-2), pp. 117-120, 1995

[34] Kim, C.B. and Su, C.B. "Measurement of the refractive index of liquids at 1.3 and 1.5 micron using a fibre optic Fresnel ratio meter." Measurement Science and Technology, vol. 15(9), pp. 1683, 2004

[35] Miki-Yoshida, M., Morales, J. and Solis, J. "Influence of Al, In, Cu, Fe and Sn dopants on the response of thin film ZnO gas sensor to ethanol vapour." Thin Solid Films, vol.373(1-2), pp. 137-140, 2000

[36] N'Konou, K., Lare, Y., Haris, M., Baneto, M., Amou, K.A. and Napo, K. "Influence of barium doping on physical properties of zinc oxide thin films synthesized by SILAR deposition technique." Advances in Materials, vol. 3(6), pp. 63-67, 2014